

中國醫藥大學

專題研究計畫成果報告

計畫名稱：探討食慾激素 B 調控 N-甲基 D-天門冬氨酸
依賴性脊髓反射增益效應之機轉

計畫編號：CMU99-S -19

執行期限：2010 年 08 月 01 日至 2011 年 07 月 31 日

單位名稱：生理學科

主持人：林則彬

中 華 民 國 年 月 日

Introduction:

SPINAL GLUTAMATERGIC N-methyl-D-aspartate (NMDA) receptor-dependent central sensitization, a form of neural plasticity characterized by the responsiveness of noxious C fibers to painful stimulation, may be dynamically enhanced following injury or inflammation and is the neural basis for hyperalgesia and allodynia. The NMDA receptor is made up of NR1-3 subunits. The NR2 subunit defines the electrophysiological properties essential for NMDA-dependent neural plasticity. Four genes encoding NR2 subunits, i.e., NR2A-D subunits, have been cloned. Evidence has revealed that NR2A- and NR2B-containing NMDA receptors play crucial roles in the induction of neural plasticity.

Lateral hypothalamic glucose-sensitive neurons, which produce orexin, orexin-A and orexin-B, have been implicated in body mass regulation. Orexin exhibits physiological functions by activating G protein-coupled orexin receptor-1 (OX-1) and OX-2, which are widely distributed in the central nervous system. Hypothalamic orexinergic fibers not only project to brain areas but also directly to the spinal cord. Although the relevance has yet to be established, electrophysiological studies suggest that orexinergic fibers descending to the dorsal horn might modulate pain processing. Electrophysiological studies suggest that orexin-A may increase NR2A-containing NMDA receptors to inhibit the NMDA-mediated EPSC (excitatory postsynaptic current) or modulate trafficking of NR2A/NR2B-containing NMDA receptors and, therefore, attenuate the induction of the NMDA-dependent form of neural plasticity.

Recently, our laboratory has reported the spinal reflex potentiation (SRP), a novel activity-dependent reflex potentiation that shares the glutamatergic NMDA receptor-dependent mechanism with spinal central sensitization. However, NMDA receptor-specific orexin modulation on SRP has not been thoroughly investigated. Therefore, we tested whether orexin is involved in the NMDA receptor-mediated SRP and the possible receptor subunits involved in the orexin-exhibited modulation.

MATERIALS AND METHODS

General Preparations

Animal care and experimental protocol were in accordance with the guidelines of the National Science Council of Taiwan, and the experimental protocol was approved by the committee of experimental animal research of Chung-Shan Medical University. All efforts were made to minimize both animal suffering and the number of animals used throughout the experiment. Fifty-three adult female Wistar rats weighing 180–350 g were anesthetized with urethane (1.2 g/kg ip). A PE-50 catheter (Portex, Hythe, Kent, UK) was placed in the left femoral vein for administration of anesthetics as needed. A midline abdominal incision was made to expose the pelvic viscera. Both ureters were ligated distally and transected proximally to the sites of ligation. The proximal ends of the ureters drained freely within the abdominal cavity. A wide-bore cannula was inserted into the lumen of the urinary bladder from a small incision made on the apex of the bladder dome and was secured with cotton thread. The open end of the cannula drained freely throughout the experiment (Fig. 1A). The right pelvic nerve was carefully dissected from the surrounding tissues and was transected distally for stimulation. The rats were monitored for a corneal reflex and a response to noxious stimulation to the paw throughout the course of the experiment. If responses were present, a supplementary dose (0.4 g/kg iv) of urethane was given through the venous catheter. When the experiments were completed, the animals were euthanized via an intravenous injection of potassium chloride saturation solution.

Intrathecal Catheter

The occipital crest of the skull was exposed, and the atlantooccipital membrane was incised at the midline with the tip of an 18-gauge needle. A PE-10 catheter was inserted through this slit and passed along the dorsal surface of the spinal cord within the intrathecal space to the dorsal intrathecal space at the L6-S1 levels of the spinal cord (Fig. 1A). The slit was then left open to avoid accumulation of intrathecal pressure caused by the injection of agents or by flushing. The volume of fluid within the cannula was kept constant at 10 ul in all experiments. A single 10-ul volume of drug solution was administered followed by a 10-ul flush of artificial cerebrospinal fluid (ACSF). It takes ~2–4 s for each 10 ul of test agent or flush injections. The location of the injection site was marked by an injection of Alcian blue (10 ul, 2%). At the end of each experiment, a laminectomy was performed to verify the location of the cannula tip. The volume of drug injected into the spinal cord in this experiment has been reported to spread from 0.5 to 1.5 mm from the site of injection as described previously. The data obtained from the experimental animals in which the cannula tip deviated by >0.5 mm from the dorsal intrathecal surface of the L6-S1 levels of the spinal cord were excluded from the statistical analysis.

Intraurethral Pressure Recording

In some experiments, to record the intraurethral pressure (IUP), two 4-0 nylon sutures were placed around the bladder trigone and ligated. A wide-bore intraurethra catheter was inserted into the urethra from the opening of the urethra. Two nylon sutures were placed above the opening of the urethra to immobilize the intraurethra catheter. The IUP was recorded continuously via the intraurethra catheter connected to a pressure transducer (P23 ID; Gould-Statham, Quincy, IL), which was connected to a computer system (Biopac, MP30, Santa Barbara, CA) through a preamplifier (Grass 7P1, Cleveland, OH).

Pelvic Nerve Stimulation

The right pelvic nerve was carefully dissected from the surrounding tissue and was transected distally. Then the central stump of the transected nerve was mounted on a pair of bipolar stainless steel wire electrodes for stimulation. Single shocks with pulse durations of 1 ms were applied to the pelvic afferent nerve from a stimulator (Grass S88) through an isolation unit (Grass SIU 5B) and a constant current unit (Grass CCU1A). Two stimulation frequencies were used in this study. The test stimulation, which is characterized by a frequency of 1/30 Hz for 180 min, was used for sampling baseline reflex activity because it did not result in response facilitation. On the other hand, the repetitive stimulation, which is characterized by a frequency of 1 Hz for 180 min, was used to induce reflex potentiation. Before the start of the experiments, test stimulation was applied to the preparation, the intensity of the stimulation was gradually increased, and a stimulus intensity that yielded a single spike action potential in reflex activity was usually chosen to standardize the stimulation intensity throughout the experiment.

Electromyogram Recording

Epoxy-coated bipolar wire electrodes (50 μ m; MT Giken, Tokyo, Japan) were placed intra-abdominally. The placement of the electrodes was performed using a 30-gauge needle with a hooked electromyogram electrode positioned at the tip (1.0–1.5 mm). To avoid the external urethra sphincter activity being contaminated by the internal sphincter and to avoid damage/obstruction in the urethra itself, the needle was inserted into the sphincter ~1–2 mm lateral to the urethra, then withdrawn, leaving the electromyogram wire embedded in the sphincter. The external urethra sphincter electromyogram (EUSE) activities were amplified 20,000-fold by a preamplifier (Grass P511AC) and then continuously displayed on an oscilloscope (Tectronics TDS 3014, Wilsonville, OR) and a recording system with a sampling rate of 20,000 Hz (MP30; Biopac, Santa Barbara, CA).

Application of Drugs

The drugs used included the following: D-2-amino-5-phosphonovalerate (APV, a glutamatergic NMDA receptor antagonist; 10 μ M, 10 l; Sigma),

6-cyano-7-nitroquinoxaline-2,4-dione [CNQX, a glutamatergic α -amino-3-hydroxy-5-methyl-4-isoxazolepropionate (AMPA) receptor antagonist; 10 μ M, 10 μ l; Sigma], glutamate (10 μ M, 10 μ l; Sigma), NMDA (10 μ M, 10 μ l; Sigma), orexin-A (an endogenous orexin receptor agonist; 3, 10, and 30 μ M, 10 μ l; Sigma), N-(6,8-difluoro-2-methyl-4-quinolinyl)-N-[4-(dimethylamino)phenyl] urea (SB-408124, a selective OX-1 antagonist; 10 μ M, 10 μ l; Sigma), (2R,4S)-4-(3-phosphonopropyl)-2-piperidinecarboxylic acid (PPPA, a selective NR2A antagonist; 30, 100, and 300 nM, 10 μ l; Tocris), and 4-hydroxy-1-[2-(4-hydroxyphenoxy)ethyl]-4-(4-methylbenzyl) piperidine (Co-101244, a selective NR2B antagonist; 3, 10, and 30 nM, 10 μ l; Tocris). Glutamate, NMDA, CNQX, APV, orexin-A, PPPA, and Co-101244 were dissolved in ACSF, whereas SB-408124 was dissolved in DMSO and applied at a final DMSO concentration of <1%. ACSF or solvent solution of identical volume to tested agents was dispensed intrathecally to serve as the vehicle.

Experimental Protocols

The schematic diagram showing the dorsal view of the arrangement of EUSE recordings in response to the afferent pelvic nerve stimulation is shown in Fig. 1A. The experimental protocols were as follows.

Protocol I: test stimulation. Single shocks repeated at 30-s intervals (1/30 Hz) were applied through the stimulation electrodes to the pelvic afferent nerve for 180 min to establish a stable baseline reflex activity.

Protocol II: repetitive stimulation. After an equilibrium period (usually 30 min), the repetitive stimulation (RS; 1 Hz, 180 min) with intensity identical to the test stimulation (TS) was applied to the pelvic afferent nerve to induce SRP.

Protocol III: glutamatergic agonists/antagonists. After protocol I or II was completed, glutamatergic agonist, glutamate or NMDA, was tested intrathecally 150 min following TS onset. On the other hand, glutamatergic NMDA or AMPA receptor antagonist, APV or CNQX, was tested intrathecally 150 min following RS onset to elucidate the possible neurotransmitters involved in SRP.

Protocol IV: NR2A and NR2B subunit antagonists. NR2A or NR2B receptor antagonist, PPPA or Co-101244, respectively, was tested intrathecally 120 min following RS onset to explore the possible subunits involved in SRP induction.

Protocol V: orexin-A and OX-1 receptor antagonists. Orexin-A was administered intrathecally 30 min following RS onset. In the experiments, which tested the effect of OX-1 antagonist, SB-408124 was injected intrathecally before application of RS to elucidate the possible receptors mediating orexin-A to modulate SRP.

Protocol VI: NR2A/NR2B antagonists and NMDA. PPPA and Co-101244 were injected intrathecally 120 min following onset of RS. NMDA was tested intrathecally 150 min after stimulation onset.

Protocol VII: orexin, NR2A/NR2B antagonists, and NMDA. Because there is, so far, no

specific NR2A- and NR2B-selective agonist available, we tested the role of NR2A and NR2B by sequential application of orexin-A (30 min following stimulation onset), PPPA or Co-101244 (120 min following stimulation onset), and NMDA (150 min following stimulation onset).

Immunohistochemistry

Immunohistochemistry was performed to assess the expression and localization of the NMDA NR2B subunit in the lumbosacral spinal cord at L6-S1 levels. Rats receiving TS, RS, and RS with an orexin-A injection (RS_OxA) were studied 180 min following stimulation onset. While under deep anesthesia (halothane-O₂), rats were perfused transcardially with saline containing 100 units heparin/ml, followed by 4% paraformaldehyde in a 0.1 M phosphate buffer (pH 7.4). Spinal segments were postfixed in 4% paraformaldehyde-0.1 M phosphate buffer for 4–5 h at 4°C before being stored in a 0.1 M phosphate buffer at 4°C. Transverse sections (70 μ m) were initially incubated in normal serum from the species that donated the secondary antibody, to block nonspecific binding. They were then incubated overnight at 4°C in a rabbit anti-NR2B polyclonal antibody (Chemicon; 1:750). All sections were then incubated in a biotinylated donkey-anti-rabbit IgG (1:200, 60 min; Chemicon), followed by incubation for another 60 min with an avidin-biotin complex solution (ABC Elite, Vector Laboratories; 1:50). After a single washing, sections were exposed to diaminobenzidine tetrachloride (DAB; 0.2 mg/ml; Sigma) in the presence of 3% hydrogen peroxide (1 μ l/ml) to enable visualizations of the precipitate. Then the sections were washed again and mounted onto poly-L-lysine-coated microscope slides (BDH), air-dried, dehydrated through ascending concentrations of alcohol, cleared in xylene (Sigma), and then mounted in DePeX (BDH). For relative quantification of immunoreactivity, an Improvision 1.44 Image Analysis Package (NIH) was used at a magnification of \times 40. Each image field was captured with the use of a charge-coupled device video camera (Sony) mounted on a Zeiss Axioscope microscope. The images were blank field adjusted to compensate for any artifacts in the camera apparatus. A standardized region of interest (80- μ m-diameter circle) cursor was aligned and consecutively centered on the mediolateral region of the lamina I-II. Arbitrary grey-scale units (in the range of 1–200) were assigned to make optimal use of the range for the given sample.

Western Blotting

Animals were decapitated after the experimental procedures were finished. The dorsal half of the spinal cord segments from L6-S1, ipsilateral to the stimulation site, was dissected, and the amount of protein was quantified. Protein samples (20 μ g) were separated on SDS-PAGE (6%) and transferred to a nitrocellulose membrane. Membranes were blocked in 5% nonfat milk and probed sequentially with antibodies against phosphorylated NR2B (1:1,000, Chemicon) and an antibody against beta-actin (1:10,000, Santa Cruz). The blots were incubated with horseradish peroxidase-conjugated antibody (1:2,000) for 1 h at room temperature and

visualized with enhanced chemiluminescence solution (5 min) followed by film exposure (2 min). Densitometric analysis of the polyvinylidene difluoride (PVDF) membranes was done with Science Lab 2003 (Fuji).

Statistical Analysis

The reflex excitability was assayed by recording the EUSE resulting from the pelvic afferent nerve stimulations. Since the single/oligounit recording technique used in this study can differentiate each action potential in the reflex activity, we therefore counted the spike number within 1 s following each shock applied instead of the integrated area under the electromyogram activity. The responses at 1, 3, 5, 10, and 30 s and at 1, 5, 10, 15, 30, 60, 90, 120, and 180 min were then off-line analyzed and plotted as a line chart, and the evoked activity at a specific time point was used to create the bar charts. Data from each specific time point were averaged from three evoked events in each animal, and then the data from all the animals in this experiment were averaged in the statistical charts. All data are presented as mean values ————— SE. Statistical analysis of the data was performed by means of ANOVA. In all cases, a difference of P 0.05 was considered statistically significant.

RESULTS

Baseline Reflex Activity and Reflex Potentiation

Initial experiments were performed in an attempt to establish a stable baseline reflex activity and the RS-induced reflex potentiation (15, 16, 48, 49). As shown in Fig. 1C, single pulses of pelvic afferent nerve TS (1/30 Hz, lasting for 180 min) evoked single action potentials, whereas an RS (at the same intensity as the TS, delivered at 1 Hz, lasting for 180 min) induced reflex potentiation in the EUSE activity. The summarized data in Fig. 1D show that the spike number evoked by each impulse averaged from 180 min following stimulation onset was significantly increased in RS compared with TS ($P < 0.01$, $n = 35$).

Glutamatergic Agonists and Antagonists

Next, we reexamined the role of glutamatergic neurotransmission in the induction of RS-induced reflex potentiation by intrathecal applications of glutamate agonists or antagonists. Because these drugs did not last for as long as 180 min, we injected these agents at 150 min following stimulation onset to verify their effects (Fig. 1B). As shown in Fig. 1C, single pulses of TS on the afferent nerve evoked single action potentials in the EUSE. Intrathecal administration of both glutamate (TS+GLU, 100 μ M, 10 μ l) and NMDA (TS+NMDA, 100 μ M, 10 μ l) at 150 min following stimulation onset induced a longer-lasting potentiation in the reflex activity. On the other hand, pelvic afferent nerve RS produced a long-lasting reflex potentiation. Intrathecal administration of both CNQX (RS+CNQX, 100 μ M, 10 μ l) and APV (RS+APV, 100 μ M, 10 μ l) at 150 min following stimulation onset inhibited the RS-induced reflex potentiation. The summarized data in Fig. 1D show that intrathecal glutamate and NMDA both significantly increased the spike number evoked by each pulse averaged from 180 min following the stimulation onset when compared with the TS alone ($P < 0.01$, $n = 35$). In addition, when compared with RS, intrathecal CNQX and APV both significantly decreased the spike numbers evoked by each stimulation ($P < 0.01$ to RS, $n = 35$).

NR2A and NR2B Antagonists

Studies have demonstrated that the subunit composition, particularly the NR2 subunits, defines the receptor properties essential for NMDA receptors to mediate synaptic efficacy. We evaluated the role of NR2A and NR2B in the induction of the RS-induced reflex potentiation by intrathecal application of PPPA (30, 100, and 300 nM, 10 μ l; all doses were tested in each animal) and Co-101244 (3, 10, and 30 nM, 10 μ l; all doses were tested in each animal), NR2A and NR2B inhibitors, respectively (Fig. 2A). As shown in Fig. 2, B and C, intrathecal PPPA slightly decreased the reflex activity evoked by the RS (RS+PPPA). Co-101244 also exhibited inhibition on the evoked activity (RS+Co), while the decrease in reflex activity was more prominent than that caused by PPPA. The inhibition on the evoked activity elicited by the RS caused by intrathecal PPPA or Co-101244 with various doses is

summarized in Fig. 2D. Intrathecal PPPA and intrathecal Co-101244 significantly decreased the spike number evoked by each impulse averaged from 180 min following stimulation onset when compared with RS alone ($P < 0.05$ and $P < 0.01$, $n = 7$ each). The decrease in spike number caused by Co-101244 demonstrated a dose-dependent manner and was significantly higher than the outcomes resulting from the PPPA ($P < 0.05$ and $P < 0.01$, $n = 7$).

Intrathecal Orexin-A

To elucidate the role of orexin in RS-induced reflex potentiation, we tested orexin-A intrathecally to verify its effect. Because pilot studies have shown that intrathecal orexin-A exhibited inhibition on the RS-induced reflex potentiation at ~30 min and obtained maximal effects at 90 min following injection, we therefore injected orexin-A intrathecally 30 min following the stimulation onset (Fig. 3A). While a stable baseline reflex activity with a single action potential was evoked by the TS, RS on the pelvic afferent nerve induced potentiation in the reflex activity. In addition, without affecting the baseline reflex activity elicited by the TS (TS+OxA), intrathecal injection of orexin-A (30 nM, 10 μ l) exhibited inhibitory effects on the RS-induced reflex potentiation at 180 min following the RS onset (RS+OxA). To further test the role of orexin-A, and to define the receptor mechanism involved in the inhibition exhibited by it, we pretreated with SB-408124 (10 μ M, 10 μ l, it), a selective OX-1 receptor antagonist, before the RS started. SB-408124 did not affect the RS-induced reflex potentiation (data not shown); however, it reversed the blocking effect on the RS-induced reflex potentiation exhibited by the orexin-A (RS+SB+OxA). Figure 3, C and D, summarizes the mean spike numbers per stimulation evoked by the TS, TS+OxA, RS, and RS+OxA with concentrations of 3, 10, and 30 nM as well as RS+OxA in association with SB-408124 pretreatment. Pretreatment with SB-408124 significantly reversed the blocking effect exhibited by orexin-A on the RS-induced reflex potentiation [$P < 0.01$ to RS+OxA (30 nM), $n = 7$].

Orexin-A and NR2A/NR2B Antagonists

The mechanism of the blocking effect of orexin-A on the RS-induced reflex potentiation was further investigated. However, since there is, so far, no specific NR2A- and NR2B-selective agonist available, we tested the role of NR2A and NR2B by pharmacological blockage using NMDA NR2A or NR2B subunit antagonist. Because the effects of NR2A and NR2B antagonists do not last as long as 120 min, which is the latency period during which intrathecal orexin-A elicited maximal effects, we administered these antagonists at 90 min following orexin injection (120 min following stimulation onset), which is the latency period during which the maximal effects of orexin-A were established. When compared, TS evoked a baseline reflex activity with a single action potential, and RS induced a reflex potentiation that was mildly attenuated by the NR2A receptor antagonist PPPA (RS+PPPA, 300 nM, 10 μ l) and was prominently inhibited by the NR2B subunit antagonist Co-101244 (RS+Co, 30 nM,

10 ul). Pharmacological activation of NMDA receptors by an intrathecal NMDA injection (10 uM, 10 ul) reversed the inhibition on RS-induced reflex potentiation caused by PPPA and Co-101244 (RS+PPPA+NMDA and RS+Co+NMDA, respectively), indicating that NMDA may reverse the inhibitory effects exhibited by NR2A and NR2B antagonists by activating NR2B- and NR2A-containing NMDA receptors, respectively. Furthermore, in Fig. 4C, co-administration of both orexin-A (30 nM, 10 l) with PPPA (RSOxAPPPA, 300 nM, 10 l) and orexin-A with Co-101244 (RSOxACo, 30 nM, 10 l) inhibited the RS-induced reflex potentiation. However, NMDA (10 M, 10 l) reversed the inhibitory effect exhibited by the co-administration of orexin-A with Co-101244 (RSOxACoNMDA) but not by the coadministration of orexin-A with PPPA (RS+OxA+PPPA+NMDA). Figure 4D summarizes the percentage of the spike numbers evoked by RS, RS+PPPA, PS+PPPA+NMDA, RS+Co, RS+Co+NMDA, RS+OxA, RS+OxA+PPPA, RS+OxA PPPA+NMDA, RS+OxA+Co, and RS+OxA+Co+NMDA. NMDA significantly reversed the inhibitory effect exhibited by RS+OxA+Co but not by RS+OxA+PPPA ($P < 0.01$ to RS+OxA+Co, $n = 7$).

Immunohistochemistry

The involvement of the NR2B subunit in the orexin-mediated inhibition of the RS-induced reflex potentiation was further investigated by immunohistochemistry studies. Figure 5 shows the immunohistochemical location of the NR2B subunit in the superficial dorsal horn at the L6, S1, and S2 segments, ipsilateral to the stimulation side, 180 min following stimulation onset. When compared with TS, RS increased the NR2B immunoreactivity in the spinal dorsal horn. This change took place selectively in the lamina I-II, ipsilateral to the stimulation side, but not in the lamina III or ventral horn. The mean optical density and the number of NR2B immunoreactive neurons at the L6 level are summarized in Fig. 5, B and C. When compared with TS, RS significantly increased the NR2B immunoactivity in both the staining intensity and the labeling frequency. However, in rats subjected to RS+OxA (30 nM, 10 ul, it) treatment, both the staining intensity and labeling frequency of NR2B immunoreactivity were reduced noticeably.

Western Blotting

To confirm the role of NR2B phosphorylation in the orexin-mediated inhibition of the RS-induced reflex potentiation, spinal tissues (dorsal half of the L6-S1 level, ipsilateral to the stimulated nerve) of rats received sham stimulation (Sham), TS, RS, RSOxA (30 nM, 10 ul), and RS+OxA in association with pretreatment with SB-408124 injections and were harvested at 180 min after stimulation onset for Western blot analysis. As shown in Fig. 6, A and C, when compared with TS, RS increased the level of total and phosphorylated NR2B (tNR2B and pNR2B, respectively); these levels had been abolished by intrathecal orexin-A. However, such an increase in tNR2B and pNR2B levels was reversed by pretreatment with SB-408124. The tNR2B and pNR2B levels induced by the sham stimulation, TS, RS, RS+OxA, and

RS+SB+OxA are summarized in Fig. 6, B and D (n = 4).

Changes in Intraurethra Pressure

To verify whether the modulation caused by orexin-A on the RS-induced pelvic-urethral reflex potentiation did affect the physiological function of the urethra, we investigated the IUP wave simultaneously with the evoked reflex activity in response to orexin-A injections. As shown in Fig. 7A, TS evoked a baseline reflex activity with single action potentials, and it was accompanied by a contraction wave in the IUP. RS produced potentiation in the reflex activity; meanwhile, the contraction wave of IUP was elongated parallel to the potentiated reflex activity. Since the simultaneous recording was not easy technically, we correlated the IUP contraction wave with the spike number evoked by stimulation. Figure 7B shows the regression line between the integrated area under the IUP wave and the spike number evoked by each pulse of RS counted within 1 s following each pulse. The r^2 of the regression line was 0.96, indicating a good correlation between the IUP contraction and evoked reflex activity. Intrathecal orexin-A (30 nM, 10 ul) exhibited no effect on the baseline reflex activity and the IUP wave elicited by the TS (TS+OxA), while it abolished the RS-induced reflex potentiation and elongated the IUP wave (RS+OxA). Pretreatment with SB-408124, a selective OX-1 antagonist, reversed the abolition of RS-induced reflex potentiation and the elongated IUP wave caused by orexin-A (RSSBOxA). Summarized data in Fig. 7C show the mean area under the IUP wave 1 s following each electric pulse in the TS, RS, TS+OxA, RS+OxA, and RS+SB+OxA. Pretreatment with SB-408124 significantly reversed the decrease caused by orexin-A in the area under the IUP wave evoked by the RS ($P < 0.01$ to RS+OxA, n = 7).

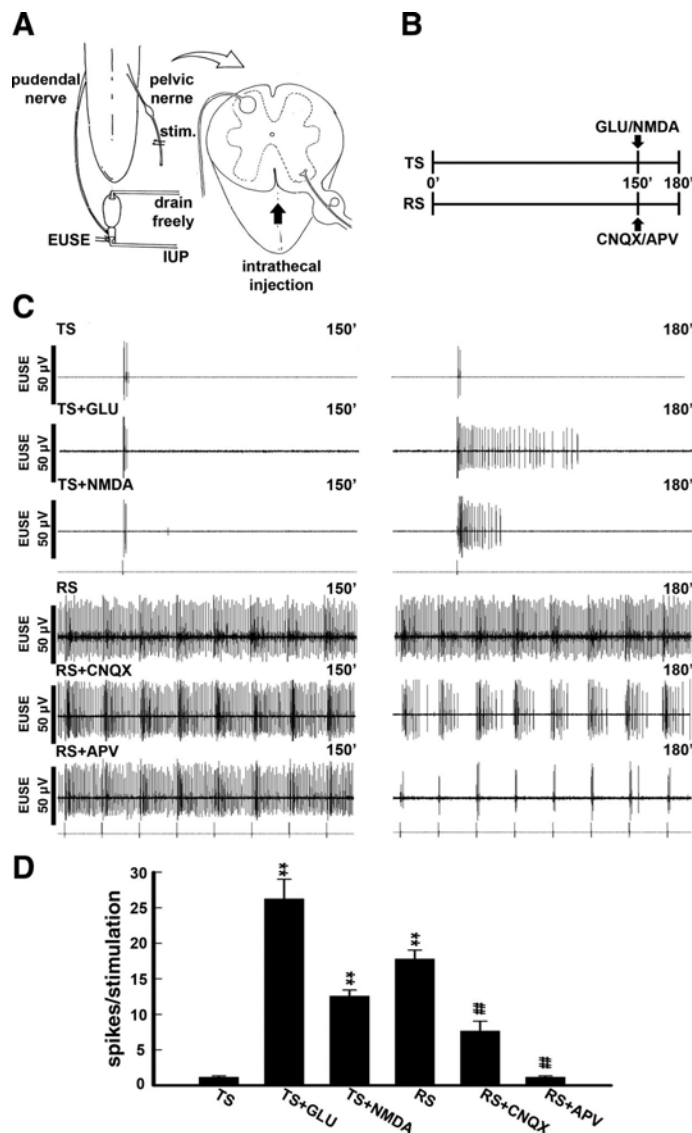


Fig. 1. Glutamate-dependent pelvic-urethral reflex potentiation. A: a schematic arrangement of the dorsal view of the spinal cord and intraurethral pressure (IUP) and external urethra sphincter electromyogram (EUSE) recordings in response to pelvic afferent nerve stimulation (Stim). B: schematic diagrams showing the schedules of experiments testing glutamatergic agonists and antagonist on the evoked activity. C: baseline reflex activity with single action potentials was evoked by test stimulation (TS). Intrathecal glutamate (TS+GLU) and NMDA (TS+NMDA) both induce potentiation in the reflex activity. Repetitive afferent nerve stimulation evoked a longer-lasting reflex potentiation (RS) that was attenuated by CNQX (RS+CNQX) and abolished by APV (RS+APV). The tracings, at left and right, show the reflex activity at the onset of and at 180 min following the stimulation, respectively. D: mean spike numbers (mean \pm SE, $n = 35$) evoked by each stimulation impulse averaged within 1 s following each shock at 180 min after stimulation onset induced by TS, TS+GLU, TS+NMDA, RS, RS+CNQX, and RS+APV. For additional abbreviation definitions, see MATERIALS AND METHODS. ** $P < 0.01$, significantly different from TS and RS, respectively. ## $P < 0.01$, significantly different from RS, respectively.

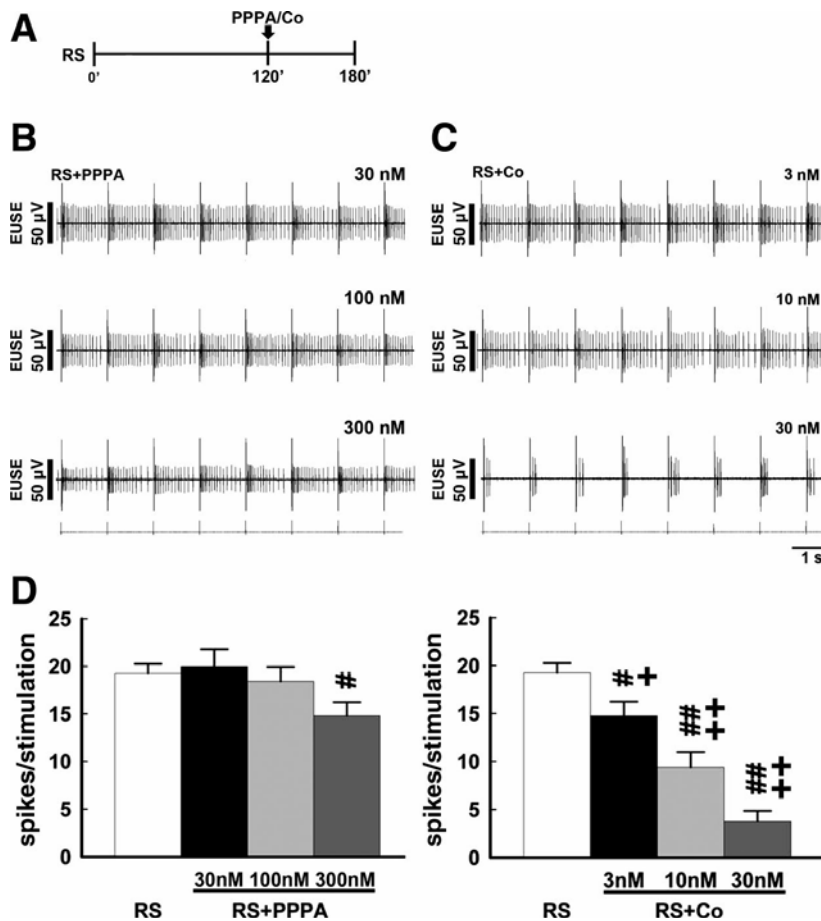


Fig. 2. Effects of NMDA NR2A and NR2B subunit antagonists on the RS-induced reflex potentiation. A: a schematic diagram showing the schedule of experiments testing NR2A and NR2B subunit antagonists. B and C: sample trace obtained from one of the test animals showing that pretreatment with PPPA (RS+PPPA) with concentrations of 30, 100, and 300 nM as well as pretreatment with Co-101244 (RS+Co) with concentrations of 3, 10, and 30 nM attenuated the RS-induced reflex potentiation. Tracings show the reflex activity at 180 min following stimulation onset. D: mean spike nos. (mean \pm SE, n = 7 each) caused by RS, RS+PPPA, and RS+Co. For additional abbreviation definitions, see MATERIALS AND METHODS. ##P < 0.01, significantly different from RS. ###P < 0.01, significantly different from RS+PPPA.

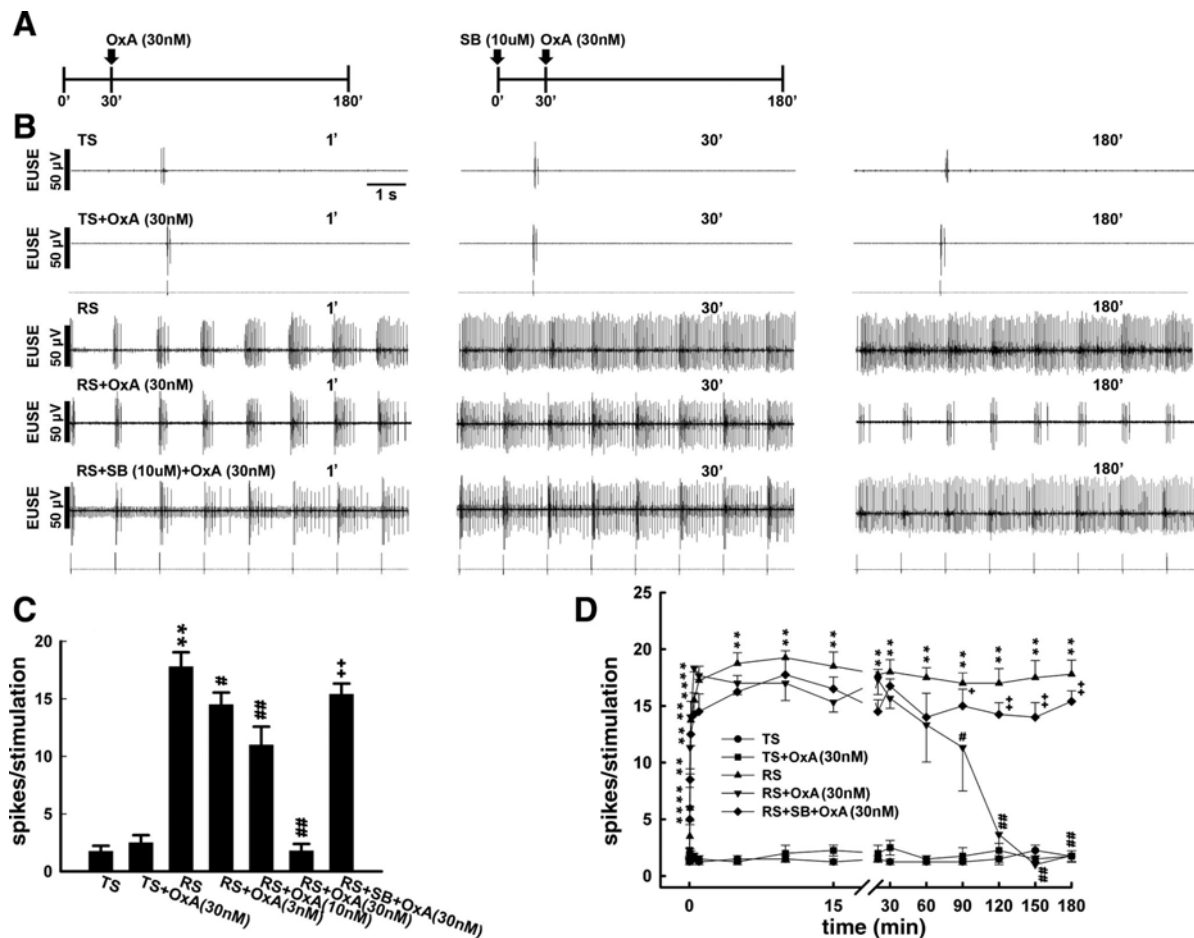


Fig. 3. Effects of orexin-A on the RS-induced reflex potentiation. A: top traces show the schematic diagram demonstrating the schedule of experiments testing orexin-A without (left) or with (right) SB-408124 pretreatment. TS evoked a baseline reflex activity with single action potentials in the EUSE, while the RS induced a long-lasting reflex potentiation. Intrathecal orexin-A (30 nM, 10 μ l) exhibited no effect on the TS-evoked baseline reflex activity, while it attenuated the RS-induced reflex potentiation (RS+OxA). An SB-408124 injection before RS onset reversed the attenuation on the reflex potentiation caused by the orexin-A (RS+SB+OxA). Left, middle, and right tracings show the reflex activity at the onset of and at 30 and 180 min following stimulation, respectively (1', 30', and 180'). B: mean spike nos. (mean \pm SE, n = 7) averaged at 180 min following stimulation onset evoked by TS, TS+OxA, RS, RS+OxA, and RS+SB+OxA. C: mean spike nos. (mean \pm SE, n = 7) averaged within 1 s following each shock during the stimulation period caused by TS, TS+OxA, RS, RS+OxA, and RS+SB+OxA. **P, ##P, and ++ P < 0.01, significantly different from activity induced by TS, RS, and RS+OxA, respectively.

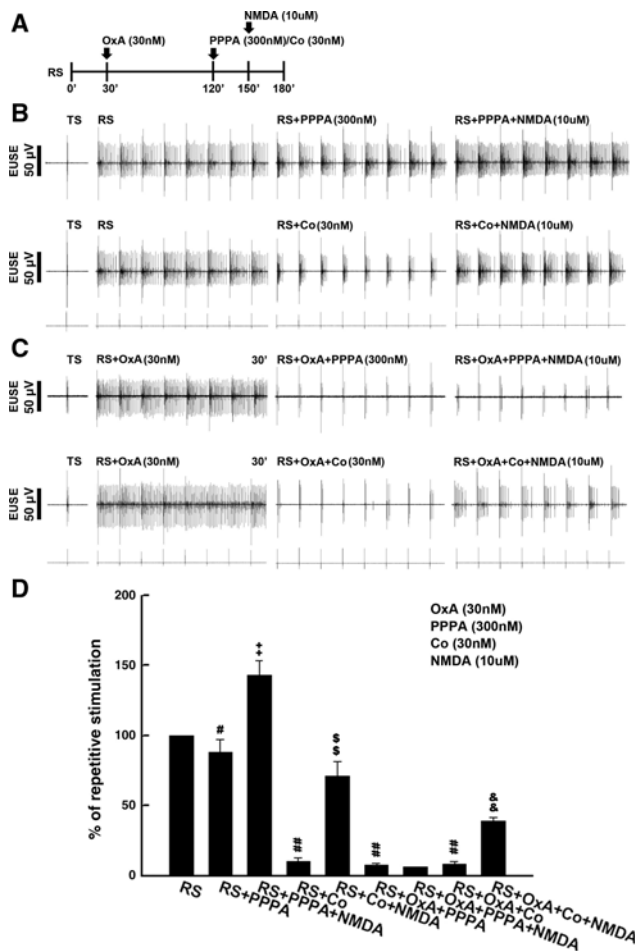


Fig. 4. Effects of orexin-A and NMDA NR2A/NR2B subunit antagonists on the RS-induced reflex potentiation. A: top traces show the schematic diagram demonstrating the schedule of the experiments testing orexin-A, PPPA/Co-101244, and NMDA. TS evoked a baseline reflex activity with a single action potential in the EUSE, whereas RS induced a long-lasting reflex potentiation. Intrathecal PPPA (RS+PPPA, 300 nM, 10 ul) and Co-101244 (RS+Co, 30 nM, 10 ul) both attenuated the RS-induced reflex potentiation. In addition, the attenuation in reflex potentiation caused by the PPPA and Co-101244 was reversed by an intrathecal NMDA (10 uM, 10 ul) injection (RS+PPPA+NMDA and RS+Co+NMDA, respectively). B: first tracing shows the reflex activity at 180 min following the TS, and the second through fourth tracings show the reflex activity at 30, 150, and 180 min following the RS onset, respectively. Co-administration of orexin-A with PPPA (RS+OxA+PPPA) and co-administration of orexin-A with Co-101244 (RS+OxA+Co) both abolished the RS-induced reflex potentiation. However, NMDA reversed the abolition caused by the co-administration of orexin-A with Co-101244 (RS+OxA+Co+NMDA) but not orexin-A with PPPA (RS+OxA+PPPA+NMDA). C: mean spike nos. (%RS, n = 7) within 1 s following each shock averaged at 180 min after stimulation onset caused by RS, RS+PPPA, RS+PPPA+NMDA, RS+Co, RS+Co+NMDA, RS+OxA, RS+OxA+PPPA+NMDA, and RS+OxA+Co+NMDA. ##P, ++P, \$\$P, and &&P < 0.01, significantly different from activity induced by RS, RS with intrathecal PPPA, RS, RS+PPPA, RS+Co, RS+OxA+PPPA, and RS+OxA+Co, respectively.

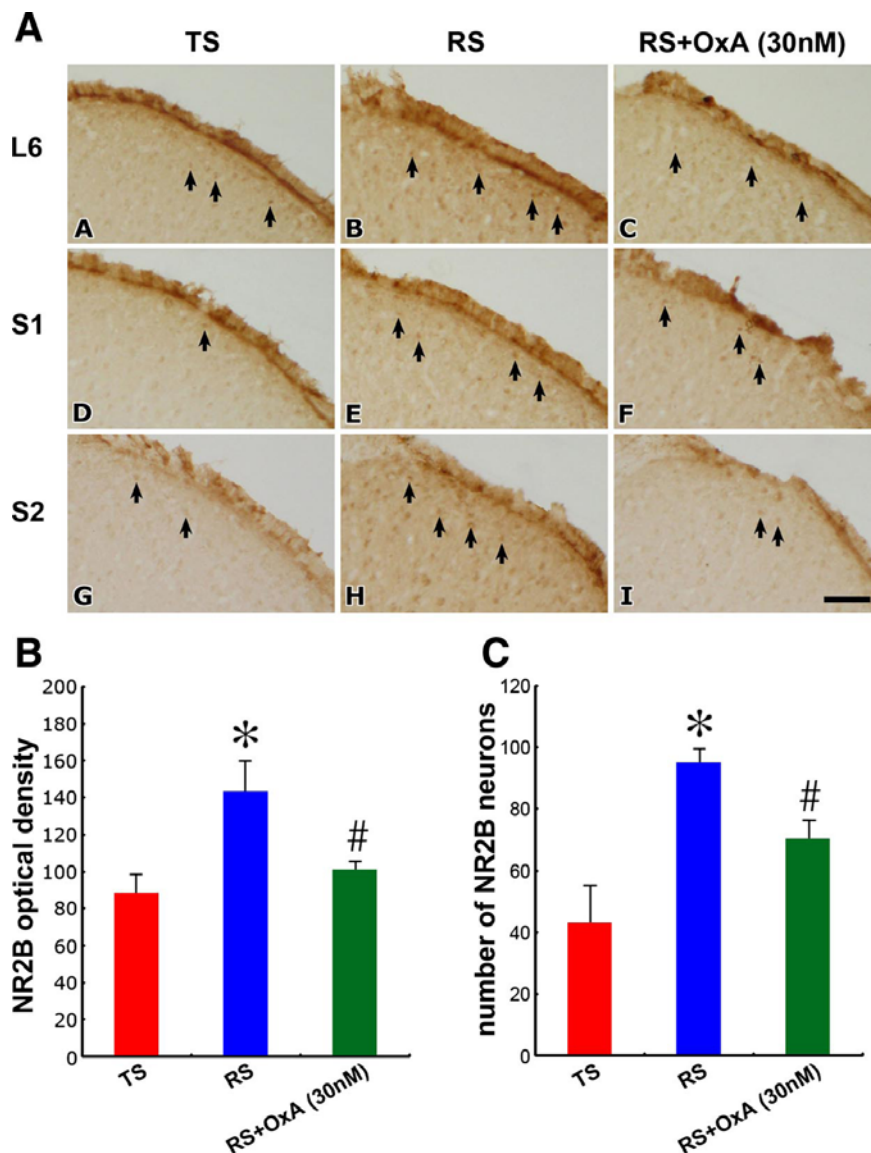


Fig. 5. Immunohistochemical analysis. A: photomicrographs showing the NR2B immunoreactivity caused by TS, RS, and RS with orexin-A (RS+OxA 30 nM) in the L6, S1, and S2 spinal cord superficial dorsal horn. In TS preparations, hardly any NR2B immunoreactive neurons (indicated by arrows) were found in the dorsal horn region, whereas in the RS group, both the staining intensity and the no. of NR2B immunoreactive neurons were drastically upregulated in the region observed (B, E, H). Conversely, pretreated orexin-A decreased the higher level of NR2B immunoreactivity in spinal segments caused by orexin-A. B and C: the mean (mean \pm SE) optical density of NR2B immunoreactivity and no. of NR2B immunoreactive neurons in the L6 spinal cord dorsal horn in rats that received TS, RS, and RS+OxA (30 nM). Note that RS significantly increased the NR2B immunoreactivity in both staining intensity and labeling frequency. However, in rats subjected to RS+OxA treatment, both staining intensity and labeling frequency of NR2B immunoreactivity reduced noticeably. Optical density of NR2B immunoreactivity correlates well with the no. of NR2B immunoreactive neurons. * $P < 0.05$ compared with TS, and # $P < 0.05$ compared with RS (n = 7).

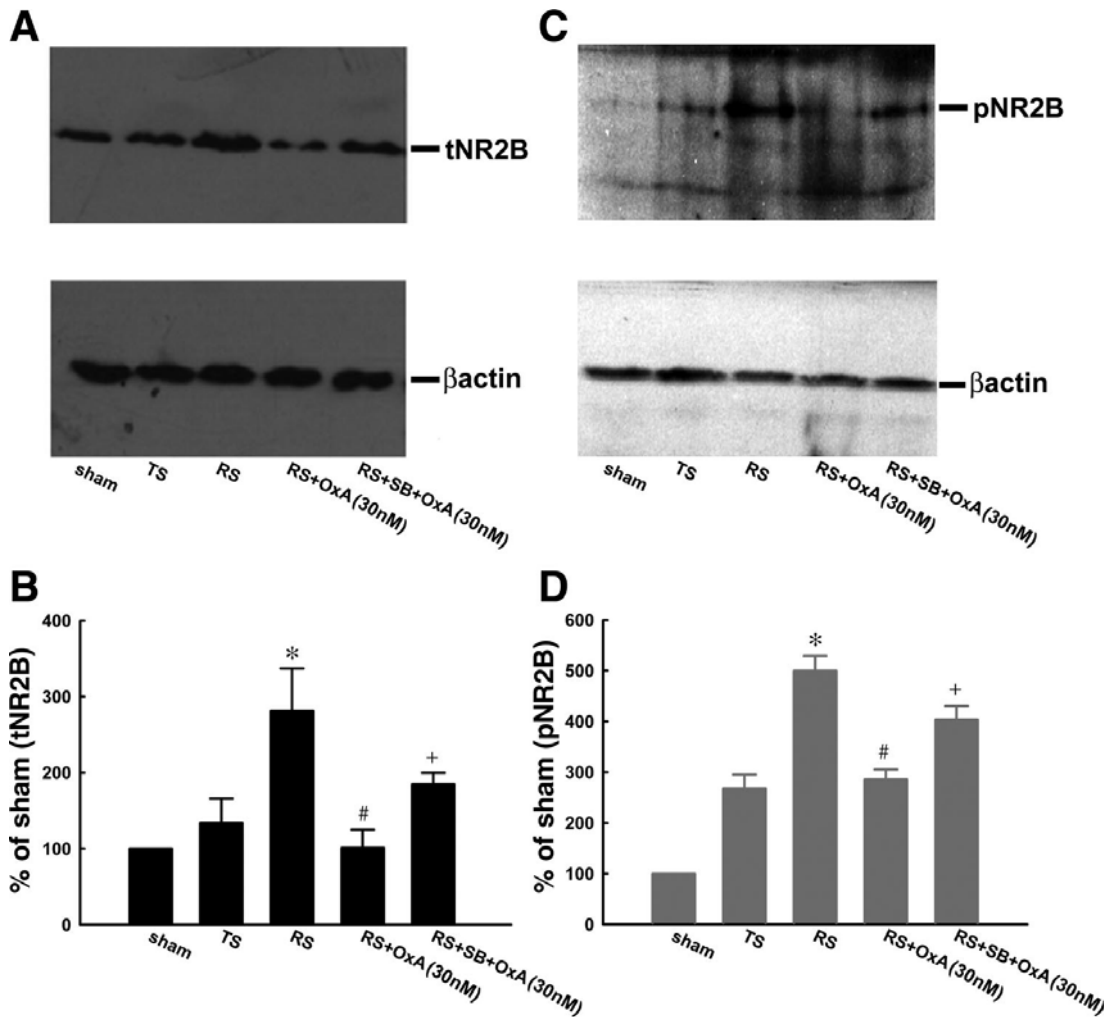


Fig. 6. Immunohistochemical and Western blotting analysis. A and C: representative Western blot showing total (tNR2B, left) and phosphorylated (pNR2B, right) NR2B expression in the protein samples of the dorsal half of the spinal cord (L6-S1), ipsilateral to the stimulation site, obtained from rats that had the sham operation (Sham) and TS, RS, RS+OxA (30 nM), and RS+SB+OxA (30 nM). B and D: summarized data showing that, when compared with pelvic NR2B immunoreactivity, which was abolished by orexin. Intrathecal SB-408124 significantly reversed the decrease in immunoactivity caused by the orexin *P < 0.05 compared with TS, #P < 0.05 compared with RS, and +P < 0.05 compared with RS+OxA (n = 4).

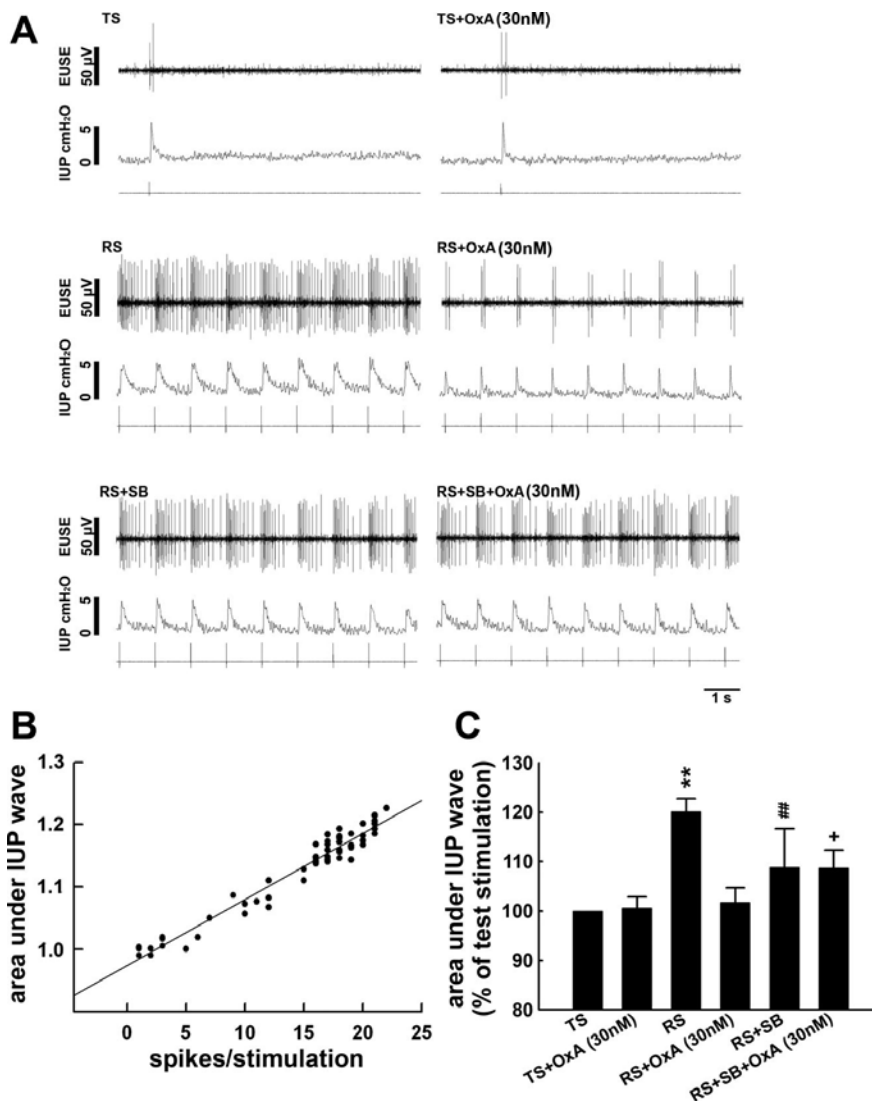


Fig. 7. Orexin-A abolished the elongation of the urethra contraction wave caused by the RS-induced reflex potentiation. A: TS evoked a baseline reflex activity with a single action potential in the EUSE in association with a contraction wave in the IUP, whereas RS induced a long-lasting reflex potentiation with an elongated IUP contraction wave. Intrathecal orexin-A exhibited no effect on the baseline reflex activity and the IUP wave evoked by the TS (TS+OxA, 30 nM), while it abolished the RS-induced reflex potentiation and the elongation of the IUP wave (RS+OxA, 30 nM). Pretreatment with SB-408124 reversed the abolition of the RS-induced reflex potentiation and the elongated IUP wave caused by orexin-A (RS+SB+OxA). Tracings show the reflex activity at 180 min following the stimulation onset. B: regression line between the area under IUP wave and the spike no. evoked by each pulse. The r^2 of the regression line was 0.96. C: mean IUP contraction intensity (mean \pm SE, $n = 7$) estimated by the area under the IUP wave 1 s following each electric shock in TS, RS, TS+OxA, RS+OxA, RS+SB, and RS+SB+OxA. Pretreatment with SB-408124 significantly reversed the decrease caused by orexin-A in the area under the IUP curve evoked by the RS. **P, ##P, and ++P < 0.01 compared with TS, RS, and RS+OxA, respectively ($n = 7$).

DISCUSSION

The dynamic regulation of reflex strength by ongoing neural activities is one of the fundamental components of central nervous system functions. In vivo studies have demonstrated that NMDA-dependent neurotransmission underlies activity-dependent SRP, and, so far, there is no other control point for SRP induction. The subunit composition of the NMDA receptor defines the receptor properties essential for the NMDA-dependent enhancement in synaptic activity. Particularly crucial are the NR2 subunits, which set the voltage dependence of the pore Mg^{2+} block and the time course of the NMDA receptor current. In the present study, pharmacological blockage using both NMDA NR2A and NR2B subunit antagonists inhibited the RS-induced SRP. Moreover, the inhibition of evoked activity exhibited by the NR2B antagonist was statistically higher than that of the NR2A antagonist. These data indicate that both NR2A and NR2B subunits are involved in the RS-induced SRP, and that NR2B seems to play a more crucial role in the induction of activity dependent SRP. This proposal is further supported by immunohistochemical experiments in this study that demonstrated that the RS significantly increased the expression of NR2B in the lamina I-II of the lumbosacral spinal cord. Our results concur with a recent study that investigated NMDA-dependent long-term potentiation (LTP) and reported that NR2B subunits played a distinct role in receptor endocytosis, which appears to be critical for the expression of enhancement in synaptic efficacy. In addition, pharmacological blockage of NR2B subunits in spinalized animal preparations has also been shown to attenuate wind-up, a spinal model of the development of central sensitization. However, a truly selective role of NR2B subunits in central sensitization, that is, spinal activity-dependent reflex potentiation, may be questionable. Following the induction of peripheral inflammation by injection of carrageenan to the hind paw or nerve injury pain by partial sciatic nerve ligation, the NR1 subunit was found to be phosphorylated on serine residues, while the NR2B expression was repressed in the rat spinal cord. These results raise the question of whether NR2B subunits contribute to spinal central sensitization. However, the data present in this study at least in part demonstrate that the phosphorylation of NR2B subunit plays a relatively dominant role in the induction of activity-dependent SRP at the spinal cord level.

Glucose-sensitive neurons in the lateral hypothalamic area produce orexin and send their axons not only to the brain area but also to the spinal dorsal horn, the area mediating nociception processing. An immunohistological study has shown that the dorsal horn area, which or the traditional roles in ingestion, metabolism, and learning, orexin may also have physiological relevance in the descending control of spinal afferent impulses triggering autonomic or somatic reflex activity underlying hypergesia or allodynia. This implication is supported by recent investigations on orexin projection, showing long descending orexinergic axonal terminals coming from the lateral hypothalamic area, innervating the superficial dorsal

horn (lamina I and II) of the spinal cord levels from the cervical to sacral segments. In addition, whole cell recording of the superficial dorsal horn neuron has demonstrated that orexin increases the spontaneous inhibitory postsynaptic current in dorsal horn neurons, indicating that electric properties of the dorsal horn neuron may be affected by orexin.

The mechanism of how orexin modulates activity-dependent reflex potentiation is still unclear. It has been suggested that orexin regulates NMDA receptor trafficking via a G protein-coupled receptor. An *in vitro* study has demonstrated that orexin-A induces potentiation of NMDA-mediated neurotransmission in the ventral tegmentum area via a PLC/PKC-dependent insertion of the NMDA receptor. Pharmacological blockage of the NMDA receptor abolishes the excitatory effect caused by orexin-A. In the present study, an intratheca NMDA injection reversed the attenuation on RS-induced SRP caused by NR2A and NR2B subunit antagonists, indicating that NMDA may reverse the inhibition by pharmacological activation of NR2B and NR2A subunits containing the NMDA receptor, respectively. However, in experiments where orexin-A was co-administrated with NR2A or NR2B antagonists, NMDA reversed the co-administration of orexin-A with NR2B but not with the NR2A antagonist. In the co-administration of orexin-A with NR2B antagonist, where the NR2B subunit was blocked by Co-101244, the subunit that was activated by the NMDA to restore SRP should have been NR2A, indicating that orexin-A did not block the NR2A subunit. On the contrary, NMDA failed to restore the SRP when there was a coadministration of orexin-A with the NR2A antagonist. Since the NR2A subunit was blocked by PPPA, the activity of NR2B should have been abolished by orexin-A. Therefore, we suggest that orexin-A may exhibit its effects on the RS-induced SRP by inhibiting the NR2B subunit. This proposal is supported by other investigations that suggest the alternation of the ratio of NR2A/NR2B-containing NMDA receptors underlies the orexin-mediated modulation on LTP, another well-known enhancement in synaptic efficacy. However, further investigation is warranted on the detailed mechanisms involved in the orexinergic inhibition on SRP.

Although the relevance of orexin in the spinal cord is still in question, studies investigating the role of orexin in pain modulation have demonstrated that orexin may attenuate headaches as well as trigeminovascular, neuropathetic, and postoperative pain. When compared with somatic pain, the complex mechanisms and pathways that contribute to the pathophysiology of visceral pain make it difficult for clinicians to treat patients. Since the RS-induced SRP, characterized by a progressive increase in responsiveness to afferent input, is quite similar to the central sensitization underlying postinflammatory hypergesia and tactile allodynia, we suggest that the descending orexinergic fibers on the spinal dorsal horn may play roles in processing visceral pain of pelvic origin by affecting the activity-dependent SRP and urethra dysynergia, which is commonly seen in patients with interstitial cystitis. The orexinergic inhibition of SRP provides an extension to the clinical situation, in which a variety of novel

targets for therapy for pelvic pain or a hyperactive urethra are now available.

The results in this study suggest that RS-induced SRP may share a glutamate NMDA-dependent neurotransmission similar to the well-investigated LTP. However, there are some obvious differences between LTP and the SRP present in this study. First, LTP is induced by high-frequency tetanic afferent input that is usually beyond 100 Hz, whereas a low-frequency stimulation paradigm (of 1 Hz) was used in this study. In addition, LTP lasts for hours after tetanization, whereas SRP decays shortly after RS cessation. In our unpublished data, the evoked activity usually recovered to the base-line level within 1 min, even if the afferent fiber was continuously stimulated with the TS following the RS offset. Furthermore, LTP applies to an increment in a single synaptic efficacy, which is typically measured by a synaptic potential rather than by action potentials, which were recorded in this study to reflect a reflex reactivity, not a monosynaptic event. Therefore, we suggest the possibility that SPR, which was inhibited by descending orexinergic innervation in the present study, is not an “LTP-like” synaptic transmission. It was noted that the SRP in this study was characterized by a gradual increase in the evoked activity following the stimulation onset. This phenomenon is similar to another well-known reflex potentiation occurring in the wide dynamic neuron in the spinal cord called wind-up. We infer that there must be some common characteristic between wind-up and SRP. However, windup, which presumably underlies postinflammatory hyperalgesia and tactile allodynia, is caused by the repetitive activation of nociceptive C fibers, while mechanical distension in the urinary bladder within the physiological range might be induced by SRP, indicating that the afferent fibers involved in these two phenomena seem to be different. In addition, wind-up is the enhancement in the responsiveness of sensory neurons, whereas SRP is the potentiation of a spinal integrated reflex activity that is recorded in the efferent pathway and the target of the reflex activity. These differences suggest that there are some substantial differences between SRP and the wind-up phenomenon. On the other hand, animal studies investigating the muscle spasticity caused by a high level spinal cord injury demonstrated an enhancement in the motoneuronal after-discharges in chronic sacral spinal cord transected preparations. Whether the SRP presented in this study correlates with the pathological enhancement in spinal reflex activity is an interesting topic that requires further investigation.

In summary, the results of this study imply that orexin, in addition to its traditional role in ingestion, metabolism, and learning, may also have physiological and pathological relevance in the descending control of spinal afferent impulses triggering autonomic reflex activity underlying hypergesia or allodynia.

REFERENCES

1. **Ahmadian G, Ju W, Liu L, Wyszynski M, Lee SH, Dunah AW, Taghibiglou C, Wang Y, Lu J, Wong TP.** Tyrosine phosphorylation of GluR2 is required for insulin-stimulated AMPA receptor endocytosis and LTD. *EMBO J* 23: 1040–1050, 2004.
2. **Aou S, Li XL, Li AJ, Oomura Y, Shiraishi T, Sasaki K, Imamura T, Wayner MJ.** Orexin-A (hypocretin-1) impairs Morris water maze performance and CA1-Schaffer collateral long-term potentiation in rats. *Neuroscience* 119: 1221–1228, 2003.
3. **Bartsch T, Levy MJ, Knight YE, Goadsby PJ.** Differential modulation of nociceptive dural input to [hypocretin] orexin A and B receptor activation in the posterior hypothalamic area. *Pain* 109: 367–378, 2004.
4. **Bekkers JM, Stevens CF.** Presynaptic mechanism for long-term potentiation in the hippocampus. *Nature* 349: 156–158, 1990.
5. **Bennett DJ, Sanelli L, Cooke CL, Harvey PJ, Gorassini MA.** Spastic long-lasting reflexes in the awake rat after sacral spinal cord injury. *J Neurophysiol* 91: 2247–2258, 2004.
6. **Berberich S, Punnakkal P, Jensen V, Pawlak V, Seeburg PH, Hvalby O, Koob GF.** Lack of NMDA receptor subtype selectivity for hippocampal long-term potentiation. *J Neurosci* 25: 6907–6910, 2005.
7. **Bernardis LL, Bellinger LL.** The lateral hypothalamic area revisited: neuroanatomy, body weight regulation, neuroendocrinology, and metabolism. *Neurosci Biobehav Rev* 17: 141–193, 1993.
8. **Bernardis LL, Bellinger LL.** The lateral hypothalamic area revisited: ingestive behavior. *Neurosci Biobehav Rev* 20: 189–287, 1996.
9. **Bingham S, Davey PT, Babbs AJ, Irving EA, Sammons MJ, Wyles M, Jefferey P, Cutler L, Riba I, Johns A.** Orexin-A, an hypothalamic peptide with analgesic properties. *Pain* 92: 81–90, 2001.
10. **Borgland SL, Taha SA, Sarti F, Fields HL, Bonci A.** Orexin A in the VTA is critical for the induction of synaptic plasticity, and behavioral sensitization to cocaine. *Neuron* 49: 589–601, 2006.
11. **Boyce S, Wyatt A, Webb JK, O'Donnell R, Mason G, Rigby M, Sirinathsinghji D, Hill RG, Rupniak NM.** Selective NMDA NR2B antagonists induce antinociception without motor dysfunction: correlation with restricted localisation of NR2B subunit in dorsal horn. *Neuropharmacology* 38: 611–623, 1999.
12. **Caudle RM, Perez FM, Del Valle-Pinero AY, Iadarola MJ.** Spinal cord NR1 serine phosphorylation and NR2B subunit suppression following peripheral inflammation. *Mol Pain* 2: 1–25, 2005.
13. **Chen GD, Peng HY, Tung KC, Cheng CL, Chen YJ, Liao JM, Ho YC, Pan SF, Chen MJ, Lin TB.** Descending facilitation of spinal NMDA-dependent reflex potentiation from

pontine tegmentum in rats. *Am J Physiol Renal Physiol* 293: F1115–F1122, 2007.

14. **Chen GD, Peng ML, Wang PY, Lee SD, Chang HM, Pan SF, Chen MJ, Tung KC, Lai CY, Lin TB.** Calcium/calmodulin-dependent kinase II mediates NO-elicited PKG activation to participate in spinal reflex potentiation in anesthetized rats. *Am J Physiol Regul Integr Comp Physiol* 294: R487–R493, 2008.
15. **Chen KJ, Chen LW, Liao JM, Chen CH, Ho YC, Ho YC, Cheng CL, Lin JJ, Huang PC, Lin TB.** Effects of a calcineurin inhibitor, tacrolimus (FK-506), on glutamate dependent potentiation in pelvic-urethral reflex in anesthetized rats. *Neuroscience* 138: 69–76, 2006.
16. **Chen KJ, Peng HY, Cheng CL, Chen CH, Liao JM, Ho YC, Liou JD, Tung KC, Hsu TH, Lin TB.** Acute unilateral ureter distension inhibits glutamate-dependent spinal pelvic-urethra reflex potentiation via GABAergic neurotransmission in anesthetized rats. *Am J Physiol Renal Physiol* 292: F1007–F1015, 2007.
17. **Cheng JK, Chou RCC, Hwang LL, Chiou LC.** Antiallodynic effects of intrathecal orexins in a rat model of postoperative pain. *J Pharmacol Exp Ther* 307: 1065–1071, 2003.
18. **Cluderay JE, Harrison DC, Hervieu GJ.** Protein distribution of the orexin-2 receptor in the rat central nervous system. *Regul Pept* 104: 131–144, 2002.
19. **Collingridge GL, Singer W.** Excitatory amino acid receptors and synaptic plasticity. *Trends Pharmacol Sci* 11: 290–296, 1990.
20. **Cull-Candy S, Brickley S, Farrant M.** NMDA receptor subunits: diversity, development and disease. *Curr Opin Neurobiol* 11: 327–335, 2001.
21. **Cutler DJ, Morris R, Sheridhar V, Wattam TA, Holmes S, Patel S, Arch JR, Wilson S, Buckingham RE, Evans ML, Leslie RA, Williams G.** Differential distribution of orexin-A and orexin-B immunoreactivity in the rat brain and spinal cord. *Peptides* 20: 1455–1470, 1999.
22. **Davis JB, Gray J, Gunthorpe MJ, Hatcher JP, Davey PT, Overend P, Harries MH, Latcham J, Clapham C, Atkinson K, Hughes SA, Rance K, Grau E, Harper AJ, Pugh PL, Rogers DC, Bingham S, Randall A, Sheardown SA.** Vanilloid receptor-1 is essential for inflammatory thermal hypergesia. *Nature* 405: 183–187, 2000.
23. **de Lecea L, Kilduff TS, Peyron C, Gao X, Foye PE, Danielson PE, Fukuhara C, Battenberg EL, Gautvik VT, Bartlett FS, Frankel WN, van den Pol AN, Bloom FE, Gautvik KM, Sutcliffe JG.** The hypocretins: hypothalamus-specific peptides with neuroexcitatory activity. *Proc Natl Acad Sci USA* 95: 322–327, 1998.
24. **Dube MG, Kalra SP, Kalra PS.** Food intake elicited by central administration of orexins/hypocretins: identification of hypothalamic sites of action. *Brain Res* 842: 473–477, 1999.
25. **Grosshans DR, Clayton DA, Coultrap SJ, Browning MD.** LTP leads to rapid surface expression of NMDA but not AMPA receptors in adult rat CA1. *Nat Neurosci* 5: 27–33,

2002.

26. **Grudt TJ, Perl ER.** Correlations between neuronal morphology and electrophysiological features in the rodent superficial dorsal horn. *J Physiol* 540: 189–207, 2002.
27. **Grudt TJ, van der Pol AN, Perl ER.** Hypocretin-2 (orexin-B) modulation of superficial dorsal horn activity in rat. *J Physiol* 538: 517–525, 2002.
28. **Gustafsson B, Wigström H.** Hippocampal long-lasting potentiation produced by pairing single volleys and brief conditioning tetani evoked in separated afferents. *J Neurosci* 6: 1575–1582, 1986.
29. **Harris GC, Aston-Jones G.** Arousal and reward: a dichotomy in orexin function. *Trends Neurosci* 29: 571–577, 2006.
30. **Hervieu GJ, Cluderay JE, Harrison DC, Roberts JC, Leslie RA.** Gene expression and protein distribution of the orexin-1 receptor in the rat brain and spinal cord. *Neuroscience* 103: 777–797, 2001.
31. **Holland PR, Akerman S, Goadsby PJ.** Orexin 1 receptor activation attenuates neurogenic dural vasodilation in an animal model of trigeminovascular nociception. *J Pharmacol Exp Ther* 315: 1380–1385, 2005.
32. **Holland P, Goadsby PJ.** Responses of hypothalamic orexin-containing neurons to cyclophosphamide, EHF irradiation of the skin, and their combination in rats. *Pathophysiology* 14: 79–85, 2007.
33. **Ji RR, Baba H, Brenner GJ, Woolf CJ.** Nociceptive-specific activation of ERK in spinal neurons contributes to pain hypersensitivity. *Nat Neurosci* 2: 1114–1119, 1999.
34. **Ji RR, Befort K, Brenner GJ, Woolf CJ.** ERK MAP kinase activation in superficial spinal cord neurons induces prodynorphin and NK-1 upregulation and contributes to persistent inflammatory pain hypersensitivity. *J Neurosci* 22: 478–485, 2002.
35. **Ji RR, Kohno T, Moore KA, Woolf CJ.** Central sensitization and long-term potentiation—do pain and memory share similar mechanisms? *Trends Neurosci* 26: 696–705, 2003.
36. **Jin SX, Zhuang ZY, Woolf CJ, Ji RR.** p38 mitogen-activated protein kinase is activated after a spinal nerve ligation in spinal cord microglia and dorsal root ganglion neurons and contributes to the generation of neuropathic pain. *J Neurosci* 23: 4017–4022, 2003.
37. **Kajiyama S, Kawamoto M, Shiraishi S, Gaus S, Matsunaga A, Suyama H, Yuge O.** Spinal orexin-1 receptors mediate anti-hyperalgesic effects of intrathecally-administered orexins in diabetic neuropathic pain model rats. *Brain Res* 1044: 76–86, 2005.
38. **Kauer JA, Malenka RC, Nicoll RA.** NMDA application potentiates synaptic transmission in the hippocampus. *Nature* 334: 250–252, 1988.
39. **Kawasaki K, Kohno T, Zhuang ZY, Brenner GJ, Wang H, Van Der Meer C, Befort K, Woolf CJ, Ji RR.** Ionotropic and metabotropic receptors, protein kinase A, protein kinase C, and Src contribute to C-fiber-induced ERK activation and cAMP response element-binding protein phosphorylation in dorsal horn neurons, leading to central

sensitization. *J Neurosci* 24: 8310–8321, 2004.

40. **Kocsis P, Kovacs G, Farkas S, Horvath C, Szombathelyi Z, Tarnawa I.** NR2B receptors are involved in the mediation of spinal segmental reflex potentials but not in the cumulative motoneuronal depolarization in vitro. *Brain Res Bull* 64: 133–138, 2004.
41. **Kopp C, Longordo F, Luthi A.** Experience-dependent changes in NMDA receptor composition at mature central synapses. *Neuropharmacology* 53: 1–9, 2007.
42. **Kovacs G, Kocsis P, Tarnawa I, Horvath C, Szombathelyi Z, Farkas S.** NR2B containing NMDA receptor dependent windup of single spinal neurons. *Neuropharmacology* 46: 23–30, 2004.
43. **Kukkonen JP, Holmqvist T, Ammoun S, Akerman KE.** Functions of the orexinergic/hypocretinergic system. *Am J Physiol Cell Physiol* 283: C1567–C1591, 2002.
44. **Lan JY, Skeberdis VA, Jover T, Grooms SY, Lin Y, Araneda RC, Zheng X, Bennett MV, Zukin RS.** Protein kinase C modulates NMDA receptor trafficking and gating. *Nat Neurosci* 4: 382–390, 2001.
45. **Lee SH, Liu L, Wang YT, Sheng M.** Clathrin adaptor AP2 and NSF interact with overlapping sites of GluR2 and play distinct roles in AMPA receptor trafficking and hippocampal LTD. *Neuron* 36: 661–674, 2002.
46. **Li Y, Harvey PJ, Li X, Bennett DJ.** Spastic long-lasting reflexes of the chronic spinal rat studied in vitro. *J Neurophysiol* 91: 2236–2246, 2004.
47. **Liao JM, Huang PC, Pan SF, Chen MJ, Tung KC, Peng HY, Shih CC, Liou YM, Chen GD, Lin TB.** Spinal glutamatergic NMDA-dependent pelvic nerve-to-external urethra sphincter reflex potentiation caused by a mechanical stimulation in anesthetized rats. *Am J Physiol Renal Physiol* 292: F1791–F1801, 2007.
48. **Liao JM, Yang CH, Cheng CL, Pan SF, Chen MJ, Huang PC, Chen GD, Tung KC, Peng HY, Lin TB.** Spinal glutamatergic NMDA-dependent cyclic pelvic nerve-to-external urethra sphincter reflex potentiation in anesthetized rats. *Am J Physiol Renal Physiol* 293: F790–F800, 2007.
49. **Lin SY, Chen GD, Liao JM, Pan SF, Chen MJ, Chen CJ, Peng HY, Ho YC, Ho YC, Huang PC, Lin JJ, Lin TB.** Estrogen modulates the spinal NMDA-mediated pelvic nerve-to-urethra reflex plasticity in rats. *Endocrinology* 147: 2956–2963, 2006.
50. **Lin TB.** Dynamic pelvic-pudendal reflex plasticity mediated by glutamate in anesthetized rats. *Neuropharmacology* 44: 163–170, 2003.
51. **Lin TB.** Tetanization-induced pelvic-to-pudendal reflex plasticity in anesthetized rat. *Am J Physiol Renal Physiol* 287: F245–F251, 2004.
52. **Liu L, Wong TP, Pozza MF, Lingenhoehl K, Wang Y, Sheng M, Auberson YP, Wang YT.** Role of NMDA receptor subtypes in governing the direction of hippocampal synaptic plasticity. *Science* 304: 1021–1024, 2004.
53. **Liu XG, Sandkuhler J.** Characterization of long-term potentiation of C-fiber-evoked potentials in spinal dorsal horn of adult rat: essential role of NK1 and NK2 receptors. *J*

Neurophysiol 78: 1973–1982, 1997.

54. **Liu XG, Sandkuhler J.** Long-term potentiation of C-fiber-evoked potentials in the rat spinal dorsal horn is prevented by spinal *N*-methyl-D-aspartic acid receptor blockage. *Neurosci Lett* 191: 43–46, 1995.
55. **Luke R, Harris W, Putman CT, Rank M, Sanelli L, Bennett DJ.** Spastic tail muscles recover from myofiber atrophy and myosin heavy chain transformations in chronic spinal rat. *J Neurophysiol* 97: 1040–1051, 2007.
56. **Luque JM, Bleuel Z, Malherbe P, Richards JG.** Alternatively spliced isoforms of the *N*-methyl-D-aspartate receptor subunit 1 are differentially distributed within the rat spinal cord. *Neuroscience* 63: 629–635, 1994.
57. **Marcus JN, Aschkenasi CJ, Lee CE, Chemelli RM, Saper CB, Yanagisawa M, Elmquist JK.** Differential expression of orexin receptors 1 and 2 in the rat brain. *J Comp Neurol* 435: 6–25, 2001.
58. **Massey PV, Johnson BE, Moulton PR, Auberson YP, Brown MW, Molnar E, Collingridge GL, Bashir ZI.** Differential roles of NR2A- and NR2B-containing NMDA receptors in cortical long-term potentiation and long-term depression. *J Neurosci* 24: 7821–7828, 2004.
59. **Morishita W, Lu W, Smith GB, Nicoll RA, Bear MF, Malenka RC.** Activation of NR2B-containing NMDA receptors is not required for NMDA receptor-dependent long-term depression. *Neuropharmacology* 52: 71–76, 2007.
60. **Pan SF, Peng HY, Chen CC, Chen MJ, Lee SD, Cheng CL, Shyu JC, Liao JM, Chen GD, Lin TB.** Nicotine-activated descending facilitation on spinal NMDA-dependent reflex potentiation from pontine tegmentum in rats. *Am J Physiol Renal Physiol* 294: F1195–F1204, 2008.
61. **Peever JH, Lai YY, Siegel JM.** Excitatory effects of hypocretin-1 (orexin-A) in the trigeminal motor nucleus are reversed by NMDA antagonism. *J Neurophysiol* 89: 2591–2600, 2003.
62. **Peng HY, Cheng YW, Lee SD, Ho YC, Chou D, Chen GD, Cheng CL, Hsu TH, Tung KC, Lin TB.** Glutamate-mediated spinal reflex potentiation involves ERK 1/2 phosphorylation in anesthetized rats. *Neuropharmacology* 54: 686–698, 2008.
63. **Petralia RS, Wang YX, Wenthold RJ.** The NMDA receptor subunits NR2A and NR2B show histological and ultrastructural localization patterns similar to those of NR1. *J Neurosci* 14: 6102–6120, 1994.
64. **Peyron C, Tighe DK, van den Pol AN, de Lecea L, Heller HC, Sutcliffe JG, Kilduff TS.** Neurons containing hypocretin (orexin) project to multiple neuronal systems. *J Neurosci* 18: 9996–10015, 1998.
65. **Prybylowski K, Wenthold RJ.** *N*-methyl-D-aspartate receptors: subunit assembly and trafficking to the synapse. *J Biol Chem* 279: 9673–9676, 2004.
66. **Sakurai T, Amemiya A, Ishii M, Matsuzaki I, Chemelli RM, Tanaka H, Williams SC,**

- Richardson JA, Kozlowski GP, Wilson S, Arch JR, Buckingham RE, Haynes AC, Carr SA, Annan RS, McNulty DE, Liu WS, Terrett JA, Elshourbagy NA, Bergsma DJ, Yanagisawa M.** Orexins and orexin receptors: a family of hypothalamic neuropeptides and G protein-coupled receptors that regulate feeding behavior. *Cell* 92: 573–585, 1998.
67. **Selbach O, Doreulee N, Bohla C, Eriksson KS, Sergeeva OA, Poelchen W, Brown RE, Haas HL.** Orexins/hypocretins cause sharp wave and θ -related synaptic plasticity in the hippocampus via glutamatergic, GABAergic, noradrenergic, and cholinergic signaling. *Neuroscience* 127: 519–528, 2004.
68. **Stephenson FA.** Subunit characterization of NMDA receptors. *Curr Drug Targets* 2: 233–239, 2001.
69. **Tigaret CM, Thalhammer A, Rast GF, Specht CG, Auberson YP, Stewart MG, Schoepfer R.** Subunit dependencies of *N*-methyl-D-aspartate (NMDA) receptor-induced alpha-amino-3-hydroxy-5-methyl-4-isoxazolepropionic acid (AMPA) receptor internalization. *Mol Pharmacol* 69: 1251–1259, 2006.
70. **Tolle TR, Berthele A, Zieglgansberger W, Seeburg PH, Wisden W.** The differential expression of 16 NMDA and non-NMDA receptor subunits in the rat spinal cord and in periaqueductal gray. *J Neurosci* 13: 5009–5028, 1993.
71. **Tong C, Conklin D, Clyne BB, Stanislaus JK, Eisenach JC.** Uterine cervical afferents in thoracolumbar dorsal root ganglia express transient receptor potential vanilloid type 1 channel and calcitonin gene-related peptide but not P2X3 receptor and somatostatin. *Anesthesiology* 104: 651–657, 2006.
72. **Trivedi P, Yu H, MacNeil DJ, Van der Ploeg LH, Guan XM.** Distribution of orexin receptor mRNA in the rat brain. *FEBS Lett* 438: 71–75, 1998.
73. **Ulfenius C, Linderoth B, Meyerson BA, Wallin J.** Spinal NMDA receptor phosphorylation correlates with the presence of neuropathic signs following peripheral nerve injury in the rat. *Neurosci Lett* 399: 85–90, 2006.
74. **van den Pol AN.** Hypothalamic hypocretin (orexin): robust innervation of the spinal cord. *J Neurosci* 19: 3171–3182, 1999.
75. **Wayner MJ, Phelix CF, Armstrong DL.** Lateral hypothalamic stimulation inhibits dentate granule cell LTP: direct connections. *Brain Res Bull* 43: 5–15, 1997.
76. **Woolf CJ.** Evidence for a central component of post-injury pain hypersensitivity. *Nature* 306: 686–688, 1983.
77. **Woolf CJ.** Generation of acute pain: central mechanisms. *Br Med Bull* 47: 523–533, 1991.
78. **Woolf CJ.** Central sensitization: uncovering the relation between pain and plasticity. *Anesthesiology* 106: 864–867, 2007.
79. **Woolf CJ, Thompson SW.** The induction and maintenance of central sensitization is dependent on *N*-methyl-D-aspartic acid receptor activation: implications for the

treatment of post-injury pain hypersensitivity states. *Pain* 44: 293–299, 1991.

80. **Yamamoto T, Nozaki-Taguchi N, Chiba T.** Analgesic effect of intrathecally administered orexin-A in the rat formalin test and in the rat hot plate test. *Br J Pharmacol* 137: 170–176, 2002.
81. **Yamamoto T, Saito O, Shono K, Aoe T, Chiba T.** Anti-mechanical allodynic effect of intrathecal and intracerebroventricular injection of orexin-A in the rat neuropathic pain model. *Neurosci Lett* 347: 183–186, 2003.
82. **Yan T, Liu B, Du D, Eisenach JC, Tong C.** Estrogen amplifies pain response to uterine cervical distension in rats by altering transient receptor potential-1 function. *Anesth Analg* 104: 1246–1250, 2007.
83. **Yung KK.** Localization of glutamate receptors in dorsal horn of rat spinal cord. *Neuroreport* 9: 1639–1644, 1998.